Detection of Fecal/Ingesta Contaminants on Poultry Processing Equipment Surfaces by Visible and Near-Infrared Reflectance Spectroscopy

K. Chao, X. Nou, Y. Liu, M. S. Kim, D. E. Chan, C.-C. Yang, J. Patel, M. Sharma

Abstract. *Visible and near-infrared (NIR) spectra and samples for laboratory microbial analysis were acquired of fecal contaminants, ingesta contaminants, and bare processing equipment surfaces (rubber and stainless steel) in a commercial poultry processing plant. Spectra were analyzed in the visible region of 450 to 748 nm and the NIR region of 920 to 1680 nm and microbial sampling for Enterobacteriaceae counts (EBC) was conducted for 82 fecal contaminant samples, 59 ingesta contaminant samples, 40 bare rubber belt areas, and 40 bare stainless steel areas. Two-wavelength band ratios in the visible and NIR regions were selected for separating contaminants from equipment areas. Principal component analysis (PCA) was performed to analyze the spectral data set and 2-class soft independent modeling of class analogy (SIMCA) models were developed for comparison with band ratio classification. Fecal and ingesta contaminants were difficult to separate from each other but both were easily differentiated from the equipment areas. The visible ratio using 518 and 576 nm correctly classified 100% of contaminant samples and 92.5% of equipment area samples. The NIR ratio using 1565 and 1645 nm correctly classified 100% of the contaminant samples and 95% of the equipment area samples. Microbiological analysis found the highest EBC levels for fecal contaminants; mean EBC for ingesta contaminants was significantly lower than that for fecal contaminants. The high EBC levels for fecal contaminants indicate that these contaminants should be targeted for spectral-based detection methods for sanitation monitoring and verification purposes; although their EBC levels are significantly lower, ingesta contaminants should also be included due to difficulty of separation from fecal contaminants.*

Keywords. *Food safety, HACCP, Sanitation monitoring, Spectroscopy.*

To ensure a wholesome and safe meat supply for consumers, the USDA Food Safety and Inspection Service (FSIS) has established policies for meat and poultry processing in order to minimize the risks of bacterial pathogens in meat and poultry products (USDA, 1994). More recently, FSIS implemented Pathogen Reduction, Hazard Analysis, and Critical Control Points (HACCP) programs, which hold processing plants accountable to detailed standard operating procedures developed by the plants to meet daily sanitation requirements (USDA, 1996). This is important to pathogen reduction because unsanitary practices in processing plants increase the likelihood of product cross contamination. Thus, plants must document daily records of completed sanitation standard operating procedures and are subject to hands-on sanitation verification by FSIS inspectors.

Because poultry feces are the most likely source of pathogenic contamination in a poultry plant, FSIS inspectors use the established guidelines to identify fecal residues on hard surfaces in the processing environment, including equipment and tools. Evaluation and inspection of sanitation effectiveness is usually performed through one or more of the following methods: human visual inspection, microbiological culture analysis, bioluminescent ATP-based assays, and antibody-based microbiological tests. However, these labor-intensive and time-consuming procedures do not meet the needs of the poultry processing industry for an accurate, high speed, and non-invasive method that can provide near immediate results that are useful for monitoring the processing line in real-time. Thus, the USDA Agricultural Research Service has been developing hyper- and multi-spectral reflectance and fluorescence imaging techniques for use in the detection of fecal material on chicken carcasses and on fresh fruit and vegetable products (Kim et al., 2003; Windham et al., 2003a; Lawrence at al., 2005; Park et al., 2005), and major developments have been achieved towards spectral imaging inspection systems for implementation on processing lines. The development of low-cost, reliable, and portable sensor systems is also being pursued, such as personal goggle and binocular devices (Ding et al., 2006), to provide affordable inspection tools to processors of all sizes. One key factor in successful applications is the use of a few essential spectral bands, which should not only reflect the chemical / physical information in the samples, but also maintain successive discrimination and

Submitted for review in April 2007 as manuscript number FPE 6990; approved for publication by the Food & Process Engineering Institute Division of ASABE in November 2007.

Mention of a product or specific equipment does not constitute a guarantee or warranty by the U.S. Department of Agriculture and does not imply its approval to the exclusion of other products that may also be suitable.

The authors are **Kuanglin Chao,** Research Scientist, **Xiangwu Nou,** Microbiologist, **Yongliang Liu,** Research Associate, **Moon S. Kim,** Research Scientist, **Diane E. Chan,** Agricultural Engineer, **Chun-Chieh Yang, ASABE Member Engineer,** Research Assoicate, **Jitu Patel,** Microbiologist,and **Manan Sharma,** Microbiologist, USDA-ARS Food Safety Laboratory, Henry A. Wallace Beltsville Agricultural Research Center, Beltsville, Maryland. **Corresponding author:** Kuanglin Chao, USDA-ARS Food Safety Laboratory, Bldg. 303, BARC-East, 10300 Baltimore Ave., Beltsville, MD 20705; phone: 301-504-8450; fax: 301-504-9466; e-mail: kevin.chao@ars.usda.gov.

classification efficiency. These essential bands can be determined through a variety of analytical strategies, such as analyzing spectral difference (Liu et al., 2003; Liu et al., 2005), performing principal component analysis (Windham et al., 2003b), and stepwise linear regression (Williams and Norris, 2001; Delwiche 2003).

The objective of this study was to find a method based on visible (VIS) or near-infrared (NIR) spectra to differentiate fecal contaminants, ingesta contaminants, and bare poultry processing equipment surfaces at a commercial poultry processing plant. Visible and NIR wavelengths were selected for band ratios to be used in classifying the contaminant and equipment samples. Principal component analysis (PCA) and 2-class SIMCA (soft independent modeling of class analogy) models were also examined for classification. Sampling and microbiological analysis of fecal contaminants, ingesta contaminants, and equipment surfaces was also performed to determine the Enterobacteriaceae counts (EBC) associated with each sample type.

Materials and Methods

In-Plant Visible and Near-Infrared Spectral Measurement and Collection of Samples

A total of 221 samples, including 141 contaminants (82 feces and 59 ingesta) and 80 bare areas (showing no visible fecal or ingesta residues) on equipment surfaces (40 samples each for bare areas on stainless steel and on rubber belt conveyors), were collected over an 8-day period at a poultry slaughter plant. All fecal and ingesta contaminant samples were scanned *in-situ* from evisceration line equipment surfaces, specifically in the areas of the rehanging conveyor belt, venting machine, and drawing machine. The size of each contaminant sample was between 5 mm to 10 mm in diameter, occupying a surface area of 0.20 to 0.78 cm^2, which fully covered the area illuminated by the probe (0.12 cm^2) for spectral measurement. Each sample was visually examined on-site by a FSIS Inspector-In-Charge and categorized as either a bare equipment surface sample or a fecal/ingesta contaminant sample.

Two portable battery-powered spectrometer systems were used to collect the reflectance spectra in the visible (400-900 nm) and NIR (900-1700 nm) regions (fig. 1). For measuring visible spectra, a EPP2000-CXR spectrometer (StellarNet Inc., Tampa, Fla.) was used with an SL1 tungsten-krypton fiber-optic light source (StellarNet Inc., Tampa, Fla.) and a R400-7-UV/VIS bifurcated fiber-optic probe (Ocean Optics Inc., Dunedin, Fla.). For measuring NIR spectra, a EPP2000-InGaAs spectrometer (StellarNet Inc., Tampa, Fla.) was used with a duplicate SL1 light source unit and a R400-7-VIS/NIR bifurcated fiber-optic probe (Ocean Optics, Dunedin, Fla.). Spectral acquisition was controlled using the manufacturer's software. The two fiber-optic probes were each made of seven optical fibers (400 μm diameter, 0.22 numerical aperture) with six illumination fibers encircling one detection fiber. Measurements were made with the use of a probe holder consisting of a non-reflective, open-bottom black box with a hole through the top to fit the fiber-optic probe. The probe holder blocked ambient light from the spectral sampling area so as to maintain consistent illumination conditions and a 1-cm probe-to-sample distance at a 45-degree measurement angle (to minimize specular effects). Before collecting sample spectra, a white reference was obtained from a 7-mm thick white Spectralon panel with nearly 99% absolute reflectance (Labsphere, Sutton, N.H.) and a dark reference was taken by pacing the optical probe 1 cm from the bottom of a black cylindrical Teflon sample cell with the light source turned off. During spectral measurement of contaminant samples, the probe holder was carefully positioned so that the probe's field of view (~0.12 cm^2) was fully illuminated within the area of the contaminant sample which ranged between 0.20 and 0.78 cm^2. For spectral measurement of bare equipment surfaces, the probe was positioned to ensure no visible contaminant residue present within the illumination area. The integration time for a single scan was 300 ms for visible measurements and 150 ms for NIR measurements. Each sample spectrum was an average of 10 scans (collected at a 2-nm interval in the visible range of 430 to 884 nm and at a 5-nm interval in the NIR range of 900 to 1700 nm) and was acquired in units of percentage of reflectance (relative reflectance) intensity (R). This data was converted to log (1/R) values and truncated into the 450- to 780-nm visible region and 920- to 1680-nm NIR region for data analysis.

Immediately following each spectral measurement, a sample for later microbial analysis was collected. Sterile specimen sponges were prepared in advance, each stored in 15 mL of buffer solution in an individual plastic specimen bag (Nasco, Whirl-Pak, Fort Atkinson, Wis.) with a unique identification number. For each contaminant sample, an unused sponge was removed from its bag, swiped across the equipment surface to collect the fecal or ingesta material, and placed back inside the plastic bag. For sampling of bare equipment surfaces, a sponge was swiped across a 50-cm^2 surface framed by a plastic template (Biotrace International Inc., USDA-050, Bothell, Wash.). The specimen bags were only identified by number; the corresponding sample type (fecal contaminant, ingesta contaminant, bare rubber surface, or bare stainless steel surface) was recorded in a separate list referenced by bag number. The specimen bags were placed in a Styrofoam shipping box with pre-frozen U-tek (-1°C) gel packs and shipped overnight for microbiological laboratory analysis the next day.

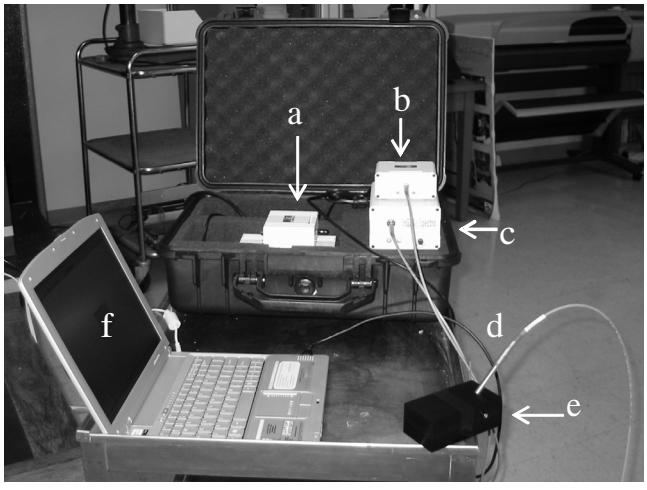

Figure 1. Components of the portable visible/near-infrared spectroscopic system: (a) battery, (b) light source, (c) spectrometer, (d) fiber-optic assembly, (e) probe holder, (f) computer.

Multivariate Data Analysis and Modeling

The following spectral preprocessing treatments were applied to all spectra: multiplicative scatter correction, mean centering, and Savitzky-Golay second derivative function with 11 smoothing points. Within each of the visible and NIR spectral sets, two classes of spectra were established: contaminant (fecal and ingesta samples) and bare equipment surface (rubber and steel samples). Approximately two-thirds of each spectral set was used for the validation data set (95 contaminant spectra and 54 bare surface spectra) and one-third was reserved for use as a test data set (46 contaminant spectra and 26 bare surface spectra).

Principal component analysis (PCA) using the PLSPlus/IQ package in Grams 32 (Version 5.2, Galactic Industries Corp., Salem, N.H.) for general characterization of the visible spectra of the four types of sample spectra was performed on all the spectral data: 82 fecal contaminant spectra, 59 ingesta contaminant spectra, 40 bare rubber surface spectra, and 40 bare stainless steel surface spectra. PCA was similarly performed to characterize the NIR sample spectra.

Using the validation data sets for the contaminant spectral class and the uncontaminated spectral class, 2-class SIMCA (Soft Independent Modeling of Class Analogy) classification was developed. One-out cross validation was used to determine the number of principal components needed per class model for achieving the minimum prediction error using the validation data sets. Mahalanobis distance calculations based on the selected models were then used to classify samples in the validation and test data sets.

Both the visible and NIR validation data sets were also analyzed to determine a simple wavelength ratio ($A\lambda_1/A\lambda_2$) by which to classify contaminant and uncontaminated sample spectra, where $A\lambda$ represents log(1/R) at wavelength λ. The 166 visible wavelengths presented 13695 possible pairwise wavelength combinations and the 153 NIR wavelengths presented 11629 possible wavelength combinations for an exhaustive search for the best visible ratio and best NIR ratio to use for classification. Using the validation data set, the SAS procedure STEPDISC (SAS Institute Inc., Cary, N.C.) was used to find potential wavelength pairs for ratio-based differentiation (Chao et al., 2003). Using both the validation and test data sets, classification of samples by ratios of these potential wavelength pairs was then examined to find the best classification ratio for each data set (visible and NIR).

Microbiological Laboratory Analysis

The samples that were collected and shipped overnight in specimen bags were processed within 4 h of receipt for microbiological laboratory analysis. For each individual bag, the contents were thoroughly mixed and three serial dilutions (100, 10^{-2}, and 10^{-4}) were prepared using buffered peptone water (BPW). One milliliter of each dilution was plated on Petrifilm#8482 Enterobacteriaceae Count Plates (3M microbiology, St. Paul, Minn.) in duplicate. After incubation at 37˚C for 18 h, characteristic Enterobacteriaceae counts (EBC) were enumerated following the guidelines provided by the manufacturer of the Petrifilm plates. The mean EBC for the four sample categories (fecal contaminant, ingesta contaminant, bare rubber belt, and bare stainless steel) were analyzed using *t*-tests (SigmaPlot 8.0, SPSS Inc., Chicago, Ill.) with statistical significance considered at *P*-values below 0.05.

Results and Discussion

Discrimination of Contaminant Samples from Background Areas Using Visible Spectra

Figure 2 shows the average log(1/R) values ± one standard deviation, for (a) fecal contaminants, (b) ingesta contaminants, (c) bare rubber belt areas, and (d) bare stainless steel areas, in the 450- to 780-nm region, which contains the color information for the samples. While the bare rubber belt and bare stainless steel surfaces consistently presented white and metallic gray appearances, respectively, the appearance of the fecal contaminant samples spanned a range of light and dark colors from yellow-orange to brown, and the colors of the ingesta contaminant samples ranged from light-green to light-yellow. Constituents from undigested feed material (such as chlorophylls and carotenoids) and constituents from the digestion process (such as bile pigments formed from dead red blood cells) contributed to the composition of the fecal and ingesta contaminant samples, which thus varied greatly in color, consistency, and texture. Consequently, distinct spectral differences can be observed between the contaminants and bare equipment surfaces. For example, both contaminant types show a similar slope in their average spectra between 500 and 600 nm, and the ingesta contaminant spectrum shows a characteristic band near 700 nm assignable to chlorophyll components. The average spectrum for bare rubber shows a broad, weak band near 600 nm. In contrast, the average spectrum for bare stainless steel lacks any notable bands between 500 and 750 nm, appearing to be quite flat. The bare stainless steel samples also tended to show the highest log(1/R) values across all wavelengths as a result of the specular character of its surface reflectance, while the more diffuse reflection of the bare rubber belt surfaces tended to result in weaker log(1/R) value across all wavelengths.

With the entire set of 221 spectra, the PLSplus/IQ package in Grams/32 was used to perform PCA. Five principal components (PCs) were found to account for 97.7% of the total variation; the first three of these explained 93.5% of that variation, with 81.1% for PC1, 8.7% for PC2, and 3.8% for PC3. The score plot in figure 3 shows that a large negative PC1 value easily separated the stainless steel samples from the other three groups, and that most of the rubber belt samples were separable from the contaminant samples by their combination of positive PC1 and negative PC2 scores. Thus, the fecal and ingesta contaminant samples were mostly separable from the equipment surfaces but were difficult to differentiate from each other, as both contaminant types were characterized by similar positive PC1 and PC2 scores.

Using the validation set of visible spectra, classification models were developed using 2-class SIMCA analysis based on contaminant and bare equipment classes. The optimal classification model was found to use three factors and two factors for the contaminant class and the equipment class, respectively. By assignment according to shorter Mahalanobis distance, the classification model identified 91% of the contaminant samples and 89% of equipment samples correctly in the cross-validation data set. When

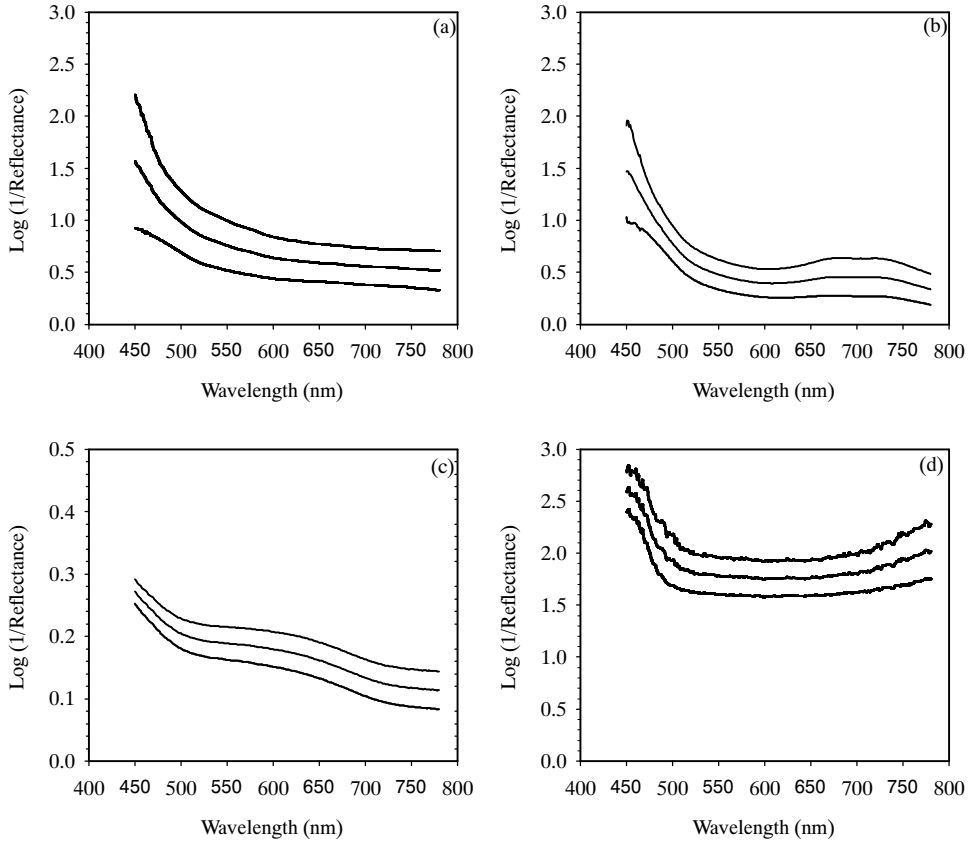

Figure 2. Average visible reflectance spectra (±1 standard deviation envelope) in the 450- to 780-nm region of (a) fecal contaminants, (b) ingesta contaminants, (c) rubber belt areas, and (d) stainless steel areas.

applied to the test data set, the model correctly classified 83% of contaminant samples and 81% of equipment samples.

Using the STEPDISC procedure, three potential visible wavelength pairs were selected for investigation, for separating the contaminant samples from the bare equipment surface samples by using threshold values of these two-wavelength ratios. Table 1 lists the classification results for these visible wavelength pairs for both the validation data set and the test data set using a threshold value of 1.15 as shown in figure 4. The wavelength pair of 518 and 576 nm achieved the highest overall separation: 100% for contaminants (above the threshold value 1.15) and 92.5% for equipment areas (below the threshold value 1.15) across the entire data set (validation and test sets combined). Only six rubber belt samples were misclassified with this wavelength pair and threshold value.

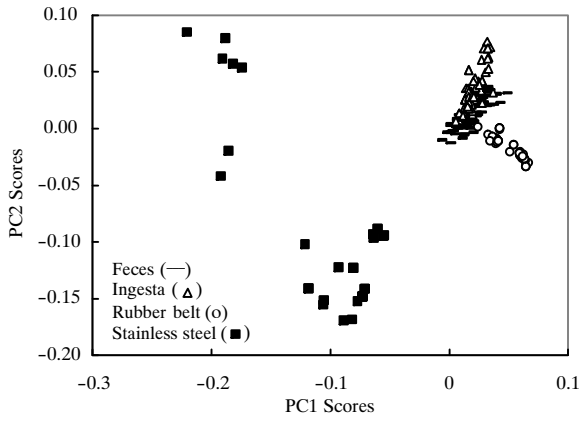

Figure 3. PC1 vs. PC2 score-score plot for visible spectra of fecal contaminants, ingesta contaminants, rubber belt areas, and stainless steel areas.

Discrimination of Contaminant Samples from Background Areas Using NIR Spectra

Figure 5 shows the average log(1/R) values ± 1 standard deviation for (a) fecal contaminants, (b) ingesta contaminants, (c) bare rubber belt areas, and (d) bare stainless steel areas, in the 920- to 1680-nm NIR region. Generally, NIR bands such as those observed for the contaminant and rubber belt areas at 980, 1195, and 1450 nm arise from first and second overtones and combinations of O-H, N-H, and C-H stretching vibrations (Osborne et al., 1993). Like the visible spectra in figure 2, the NIR spectra in figure 5 show that the stainless steel areas had the highest log(1/R) values, followed by the fecal contaminant, ingesta

Table 1. Selected visible and NIR wavelength pairs for band-ratio classification of contaminant and equipment samples in the validation and test data sets.

Classification by Two-Wavelength Band-Ratio, $A_{\lambda1}/A_{\lambda2}$					
Visible Band Ratios			Near-Infrared Band Ratios		
λ1, λ2 (nm)	Validation (%)	Test (%)	λ1, λ2 (nm)	Validation (%)	Test (%)
518, 576	97.3	97.2	1565, 1645	98.6	97.2
470, 590	95.3	93.0	1500, 1665	98.6	95.8
450, 700	90.6	88.9	1450, 1670	95.3	95.8

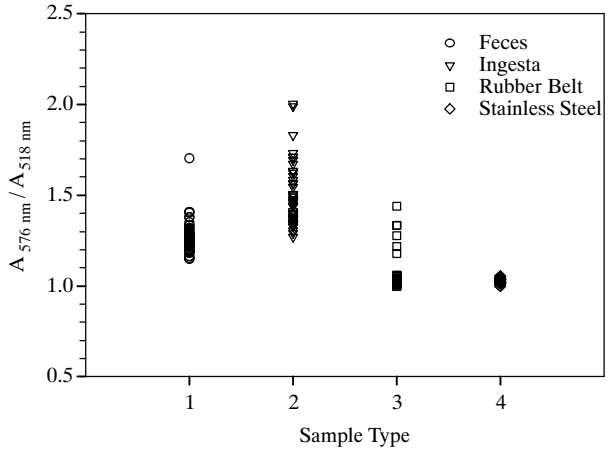

Figure 4. Visible band ratio values for classification by $A_{518\ nm}/A_{576\ nm}$, for (1) fecal contaminants, (2) ingesta contaminants, (3) rubber belt areas, and (4) stainless steel areas.

contaminant, and rubber belt areas. Again, the stainless steel exhibited a relatively flat spectrum with no obvious band characteristics except for the noise-related features at the beginning and end of the spectrum. The bare rubber belt spectra show the lowest overall log(1/R) values and also a band feature near 1665 nm that contributes to a spectral profile between 1500 and 1680 quite distinct from that of the fecal and ingesta contaminant spectra, which show decreases in log(1/R) values between 1500 and 1680 nm similar to each other.

PCA was again performed, using the entire set of 221 NIR spectra. Three PCs were found to account for 98.3% of the total variation; the first two PCs explained over 97.0% of that variation, with 87.0% for PC1 and 10.0% for PC2. Due to large positive PC1 scores, the stainless steel group was clearly isolated from the other three groups. The score plot in figure 6 shows that, with the three remaining groups, an appropriately chosen negative PC1 value near –0.022 can separate most of the rubber belt samples from the ingesta contaminant and fecal contaminant samples. The two contaminant groups, however, could not be clearly separated using PC1 or PC2 values.

Using the validation set of NIR spectra, classification models were developed using 2-class SIMCA analysis based on contaminant and bare equipment classes. The optimal classification model was found to use two factors and three factors for the contaminant class and the equipment class, respectively. By assignment according to shorter Mahalanobis distance, the classification model correctly identified 82% of the contaminant samples and 85% of equipment samples in the validation data set. When applied to the test data set, the model correctly classified 87% of contaminant samples and 77% of equipment samples.

Using the STEPDISC procedure, three potential NIR wavelength pairs were selected for investigation, for separating the contaminant samples from the bare equipment surface samples by using threshold values of these two-wavelength ratios. Table 1 lists the classification results for these wavelength pairs for both the validation data set and the test data set using a threshold value of 1.08 as shown in figure 7. The wavelength pair of 1565 and 1645 nm achieved the highest overall separation: 100% for contaminants (above the threshold value 1.08) and 95.0% for equipment areas (below the threshold value 1.08) across the entire data set (validation and test sets combined), with only four rubber belt samples misclassified.

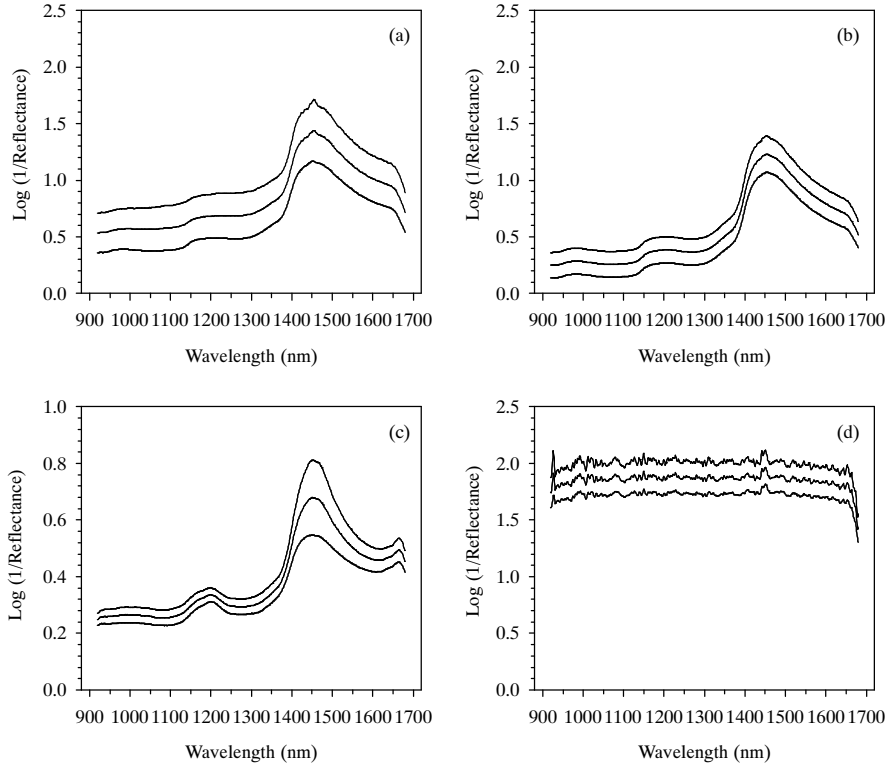

Figure 5. Average NIR reflectance spectra (±1 standard deviation envelope) in the 920- to 1680-nm region of (a) fecal contaminants, (b) ingesta contaminants, (c) rubber belt areas, and (d) stainless steel areas.

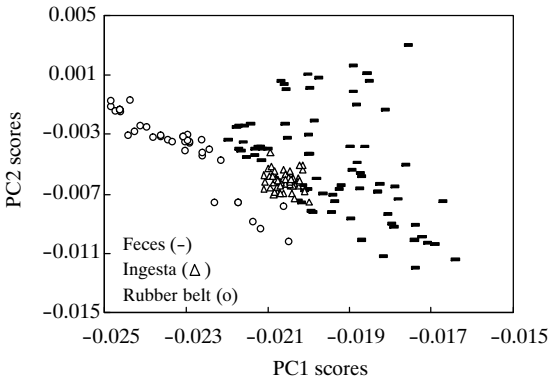

Figure 6. PC1 vs. PC2 score-score plot for NIR spectra of fecal contaminants, ingesta contaminants, and rubber belt areas.

Bacterial Counts from Microbiological Sample Analysis

The mean EBC ($\log_{10}$ cfu/mL), ± standard error of measurement, for the four sample categories were found to be 4.2903 ± 0.0829 for fecal contaminants (n = 82), 0.1886 ± 0.0421 for ingesta contaminants (n = 59), 0.0940 ± 0.0157 for bare rubber areas (n = 40), and 0.0516 ± 0.0199 for stainless steel areas (n = 40). These mean EBC values were compared, in pairs, using a t-test with significance levels of $P < 0.05$. The fecal contaminant EBC was found to be significantly higher than the EBC for each of the other three categories. The ingesta contaminant EBC was significantly different from the stainless steel EBC (P = 0.022), but not from rubber belt EBC (P = 0.059). The rubber belt EBC and stainless steel EBC were not significantly different (P = 0.095).

Comparison of the low EBC for ingesta contaminants to the higher EBC for fecal contaminants, as shown in figure 8, suggest that ingesta contaminants do not present the same food safety risks as fecal contaminants do. However, since ingesta contaminants visually resemble fecal contaminants, ingesta contaminants are more safely considered as a contaminant for food safety purposes of spectral contaminant detection for sanitation monitoring. Compared to the rubber belt EBC values, the slightly lower EBC values for stainless steel surfaces may result from steel being easier to clean and disinfect than polymeric and rubber surfaces (Krysinski et al., 1992; Ronner and Wong, 1993).

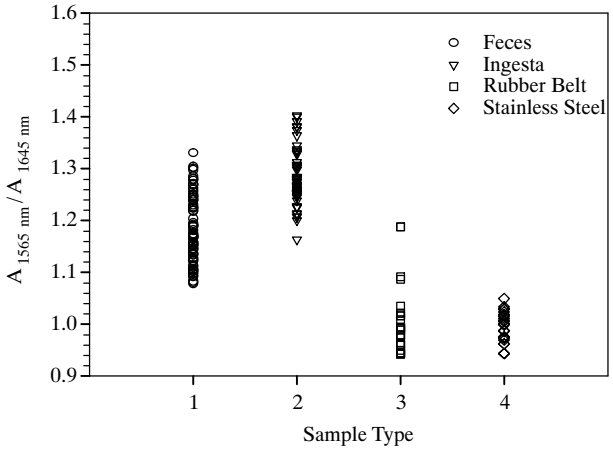

Figure 7. Near-infrared band ratio values for the classification by $A_{1565\ nm}/A_{1645\ nm}$, for (1) fecal contaminants, (2) ingesta contaminants, (3) rubber belt areas, and (4) stainless steel areas.

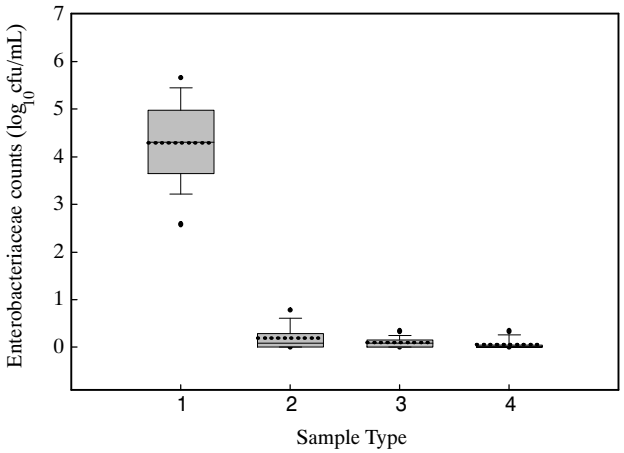

Figure 8. Enterobacteriaceae counts (EBC) for (1) fecal contaminants, (2) ingesta contaminants, (3) rubber belt areas, and (4) stainless steel areas.

Conclusions

This study found that the visible band ratio using the 518- and 576-nm wavelength pair and the NIR band ratio using the 1565- and 1645-nm wavelength pair were both able to identify 100% of fecal and ingesta contaminants. The bare stainless steel surfaces were easily differentiated from the contaminant samples, but a small percentage of bare rubber belt surfaces were misclassified by both the visible and NIR band ratios. The NIR ratio performed slightly better, achieving 95.0% correct identification for bare equipment surfaces, while the visible ratio achieved 92.5%. Both band ratios performed better in separating contaminants from equipment surfaces than did visible and NIR SIMCA models. Microbiological analysis of contaminant and equipment surface samples showed significant EBC values for fecal contaminant samples, compared to the other three sample types. Compared to fecal contaminants, ingesta contaminants showed significantly lower EBC values, but were not easily differentiated spectrally. Consequently, for the development of a device implementing these Vis/NIR waveband ratios for rapid and accurate surface sanitation verification purposes, fecal and ingesta contaminants should be included together for target detection.

References

Chao, K., Y. R. Chen, and D. E. Chan. 2003. Analysis of Vis/NIR spectral variations of wholesome, septicemia, and cadaver chicken samples. *Applied Engineering in Agriculture* 19(4): 453-458.

Delwiche, S. R. 2003. Classification of scab- and other mold-damaged wheat kernels by near-infrared reflectance spectroscopy. *Transactions of the ASAE* 46(3): 731-738.

Ding, F., Y. R. Chen, K. Chao, and M. S. Kim. 2006. Three-color mixing for classifying agricultural products for safety and quality. *Appl. Optics.* 45(15): 3516-3526.

Kim, M. S., A. M. Lefcourt, and Y. R. Chen. 2003. Multispectral laser-induced fluorescence imaging system for large biological samples. *Appl. Optics.* 42(19): 3927-3943.

Krysinski, E. P., L. J., Brown, and T. J. Marchisello. 1992. Effect of cleaners and sanitizers on Listeria monocytogenes attached to product contact surfaces. *J. of Food Protection* 55(3): 246-251.

Lawrence, K. C., W. R. Windham, D. P. Smith, B. Park, and P. W. Feldner. 2005. Effect of broiler carcasses washing on fecal contaminant imaging. *Transactions of the ASABE* 49(1): 133-141.

Liu, Y., W. R. Windham, K. C. Lawrence, and B. Park. 2003. Simple algorithms for the classification of visible/near-infrared and hyperspectral imaging spectra of chicken skins, feces, and fecal contaminated skins. *Appl. Spectr.* 57(12): 1609-1612.

Liu, Y., Y. R. Chen, C. Y. Wang, D. E. Chan, and M. S. Kim. 2005. Development of a simple algorithm for the detection of chilling injury in cucumbers from visible/near-infrared hyperspectral imaging. *Appl. Spectr.* 59(1): 78-85.

Osborne, B. G., T. Fearn, and P. H. Hindle. 1993. *Practical Near-Infrared Spectroscopy with Application in Food and Beverage Analysis*. Harlow, UK: Longman Scientific & Technical.

Park, B., K. C. Lawrence, W. R. Windham, and D. P. Smith. 2005. Multispectral imaging system for fecal and ingesta detection on poultry carcasses. *J. Food Proc. Engr.* 27(5):311-327.

Ronner, A. B., and A. C. L. Wong. 1993. Biofilm development and sanitizer inactivation of Listeria monocytogenes and Salmonella typhimurium on stainless steel and Bunna-n rubber. *J. Food Protection* 56(6): 750-758.

USDA. 1994. Enhanced poultry inspection. Proposed rule. Fed. Reg. 59:35659. Washington D.C.: USDA.

USDA. 1996. Pathogen reduction, hazard analysis and critical control point (HACCP) systems. Final Rule. Fed. Reg. 61:28805-38855. Washington D.C.: USDA.

Williams, F., and K. Norris. 2001. *Near-Infrared Technology in the Agricultural and Food Industries*. St. Paul, Minn.: American Association of Cereal Chemists.

Windham, W. R., D. P. Smith, B. Park, K. C. Lawrence, and P. W. Feldner. 2003a. Algorithm development with visible/near-infrared spectra for detection of poultry feces and ingesta. *Transactions of the ASAE* 46(6): 1733-1738.

Windham, W. R., K. C. Lawrence, B. Park, and R. J. Buhr. 2003b. Visible/NIR spectroscopy for characterizing fecal contamination of chicken carcasses. *Transactions of the ASAE* 46(3): 747-751.